Bone Reports 5 (2016) 62–69

Contents lists available at ScienceDirect

Bone Reports

journal homepage: www.elsevier.com/locate/bonr

Effects of odanacatib on bone matrix mineralization in rhesus monkeys are similar to those of alendronate

Barbara M. Misof [a,*], Paul Roschger [a], Charles Chen [b], Maureen Pickarski [b], Phaedra Messmer [a], Klaus Klaushofer [a], Le T. Duong [b]

[a] Ludwig Boltzmann Institute of Osteology at the Hanusch Hospital of WGKK and AUVA Trauma Centre Meidling, 1st Medical Department, Hanusch Hospital, Vienna, Austria
[b] Merck Research Laboratories, West Point, PA 19486, USA

ARTICLE INFO

Article history:
Received 10 February 2016
Accepted 3 March 2016
Available online 6 March 2016

Keywords:
Cathepsin K inhibitor
Odanacatib
Alendronate
Bone quality
Osteoporosis

ABSTRACT

Odanacatib (ODN) is a selective and reversible inhibitor of cathepsin K which is an important enzyme for the degradation of collagen I. Aim of the present work was the head-to-head comparison between the effects of ODN and alendronate (ALN) on bone mineralization density distribution (BMDD), based on quantitative backscattered electron imaging in relation to changes in histomorphometric mineralizing surface per bone surface (MS/BS) in 12–22 years old ovariectomized rhesus monkeys. Trabecular and cortical BMDD derived parameters from vertebrae and proximal tibiae were compared among vehicle (VEH, n = 8), odanacatib low dose (ODN-L, n = 8), odanacatib high dose (ODN-H, n = 8), and alendronate (ALN, n = 6) treated animals. Additionally, data from an intact, non-treated group of animals are shown (INT, n = 8). In trabecular bone from the vertebra and metaphyseal tibia, the BMDD of the ODN and ALN treatment groups was shifted toward higher mineralization densities ($p < 0.001$) consistent with the significant reduction of MS/BS ($p < 0.05$ in ODN-H and ALN) compared to VEH. Vertebral trabecular CaMean (average degree of mineralization) was significantly higher in ODN-L (+6.5%), ODN-H (+6.1%), and ALN (+6.7%, all $p < 0.001$). Tibial osteonal cortical bone revealed also significantly increased CaMean for ODN-L (+1.4%, $p < 0.05$), ODN-H (+2.2%, $p < 0.05$), and ALN (+3.4%, $p < 0.001$) versus VEH, while primary cortical bone (devoid of secondary osteons) did not show any significant differences between the study groups. The percentage of primary bone area in the tibial cross-sections (on average 45 ± 12%) was also not significantly different between the study groups ($p = 0.232$). No significant differences in any BMDD parameters of all studied skeletal sites between ODN and ALN treatment were found. Correlation analysis revealed that MS/BS was highly predictive for trabecular BMDD in vertebral bone. The higher MS/BS, the lower was CaMean. Our findings are consistent with the inhibition of bone resorption of ODN and ALN in trabecular and osteonal compartments.

1. Introduction

Odanacatib (ODN) is a selective and reversible inhibitor of cathepsin K which is an important enzyme for the degradation of collagen I by osteoclasts (Duong, 2012) and has been developed for its use in high bone turnover diseases such as postmenopausal osteoporosis (Reginster et al., 2014). The efficacy of ODN at different formulae and doses was shown in numerous preclinical animal studies. In estrogen-deficient rabbits, ODN prevented bone loss (Pennypacker et al., 2011) and had different effects compared to ALN as shown by histomorphometry (Jensen et al., 2014). Studies on ovariectomized rhesus monkeys (Masarachia et al., 2012; Williams et al., 2013) reported that ODN reduced trabecular bone turnover and increased bone mineral density (BMD) in a dose-dependent manner. Furthermore, it increased femoral cortical width due to preservation of endocortical bone formation rate and increase in periosteal bone apposition in OVX rhesus monkeys (Cusick et al., 2012; Cabal et al., 2013; Pennypacker et al., 2014). Phase III trials have confirmed that ODN treatment increased BMD in lumbar spine and total hip in postmenopausal osteoporotic patients (Chapurlat, 2015). In particular, increases in cortical thickness, area and estimates of finite element analysis-derived strength at radius, tibia and hip were described after ODN treatment in postmenopausal osteoporotic women (Brixen et al., 2013; Cheung et al., 2014). Long-term effects of ODN at 50-mg once-weekly in patients are currently studied in the phase III Long-Term ODN Fracture Trial (LOFT) (Bone et al., 2015). Duong et al. recently summarized all ODN trials (Duong et al., 2015).

Information of bone material quality after ODN treatment is sparse. Among the bone quality parameters, the degree and heterogeneity of bone mineralization are important determinants for the intrinsic

* Corresponding author at: Ludwig Boltzmann Institute of Osteology, UKH Meidling, Kundratstr. 37, A-1120 Vienna, Austria.
E-mail address: barbara.misof@osteologie.at (B.M. Misof).

http://dx.doi.org/10.1016/j.bonr.2016.03.001

elasticity/stiffness and other mechanical properties of the bone material (Currey, 2004; Fratzl et al., 2004). In particular, the assessment of potential treatment effects on bone matrix mineralization is an important aspect of the general evaluation of treatment-related assessments of bone quality. In the present study, bone matrix mineralization properties were investigated at the micron structural level using quantitative backscatter electron imaging (qBEI) (Roschger et al., 2008). Employing this method, the degree of mineralization (the mineral content of the bone matrix) and its spatial distribution as well as its heterogeneity within the bone tissue can be determined. Thus, this method allows detection of the degree of mineralization, independent of bone volume.

In the current prevention mode study, ovariectomized non-human primates were treated with two doses of odanacatib (ODN) of a new formulation. We previously reported at oral administration of ODN at 6 and 30 mg/kg/day in the conventional methocel formulation provided subclinical exposures (2 and 4 μM-hr_{0-24}) in monkeys (Cusick et al., 2012). These subclinical ODN doses did not affect bone matrix mineralization significantly as reported previously (Fratzl-Zelman et al., 2013). Trends of dose-dependent shifts toward higher bone matrix mineralization with ODN could be observed, and the effect was more pronounced at sites with higher remodeling rates (Fratzl-Zelman et al., 2013). To investigate the bone safety profile of ODN, a second study in rhesus monkeys was carried out with doses higher than the clinical exposure of ODN (6–7 μM-hr_{0-24}) as estimated from the 50-mg once-weekly dose in humans (Stoch et al., 2009). Two doses of ODN were administered orally daily to OVX-rhesus monkeys for 20-months using a novel formulation that achieved steady state drug exposures at ~1.8 (ODN-L) and ~7.8-fold (ODN-H) of the clinical exposure (Williams et al., 2013). These were compared to alendronate (ALN) subcutaneous dose selected to produce a plasma concentration approximate to the 70-mg oral once-weekly dose in human (Thompson et al., 1992). The aim of the present study was to measure the BMDD at trabecular and cortical sites after 20 months of treatment with two different doses of ODN treated and to compare the results head to head with alendronate (ALN) and vehicle (VEH) treatment. For additional information, BMDD of untreated, not ovariectomized animals (INT) was analyzed. Furthermore, mineralizing bone surface per bone surface, a primary histomorphometric index of bone formation, was assessed for supporting of the interpretation of the bone matrix mineralization outcomes.

2. Material and methods

2.1. Study design

All procedures were approved by the Institutional Animal Care and Use Committee of Merck Research Laboratories. Sixty-four female rhesus monkeys (*Macaca mulatta* 12–22 years of age) were randomized into four groups as previously described (Williams et al., 2013). Following bilateral OVX, the groups received the following treatments: (i) Vehicle (VEH) containing the enhanced formulation hydroxypropyl methyl cellulose acetate succinate (HPMC-AS) polymer; (ii) ODN at 2 mg/kg, (ODN-L, p.o., q.d.); (iii) ODN at 4 mg/kg (ODN-H, p.o., q.d.); (iv) ALN at 30 μg/kg/week (15 μg/kg twice weekly, s.c.). Drug treatment was initiated in prevention mode, approximately 10-days post-surgery. ALN at 15 μg/kg twice weekly, s.c. was approximately the i.v. dose of 50 μg/kg every two weeks, which was previously demonstrated to fully protect estrogen-deficiency induced bone loss in OVX baboons (Thompson et al., 1992). Compared to the daily clinical exposure of 6–7 μM·hr_{0-24} estimated from the ODN 50-mg once-weekly dose, the 24 h plasma exposure (AUC_{0-24}) for the ODN-L (2 mg/kg/d) dosed in HPMC-AS formulation was ~12 μM·hr_{0-24} in monkey. ODN-H group was initially dosed with ODN 8 mg/kg/d, progressively resulting in a drug concentration of 142 μM·hr_{0-24}; hence, this dose group was subsequently reduced to 4 mg/kg/d after 5.5 months, to maintain plasma exposure of ODN at 51 μM·hr_{0-24} for the rest of the study duration. For additional information, samples of a separate group of aged and body weight matched intact (INT) animals (outside the study groups) which were not ovariectomized and remained untreated were analyzed and outcomes are shown.

The study groups were maintained on a high protein diet (19.8%) containing 1.17% Ca, 0.7% P, 8 IU/g vitamin D3 diet (Harlan Teklad 8773 NIB primate diet ~200 g/d). To obtain dynamic histomorphometric measurements of the bone forming surfaces, double fluorochrome labels with a 15-day or 14-day interval were administered at two different time points during the study: calcein (CAL, 12 mg/kg, s.c.) at month 12, and tetracycline (TCY, 40 mg/kg, i.v.) at month 20, respectively.

2.2. Bone samples

A total of 30 samples (n = 8 VEH, n = 8 ODN-L, n = 8 ODN-H, and n = 6 ALN) were randomly selected from the four treatment groups for material level measurements of BMDD using qBEI. Additionally samples from n = 8 INT were measured. Lumbar vertebrae 6 (LV6) were dissected at necropsy and halved frontally after gentle removal of soft tissue; the ventral plane was retained for analysis. Tibiae were disarticulated from femora and adherent tissues gently removed. Using a band saw (Exakt band system 300/CP; Exakt Advanced Technologies, GmbH Norderstedt, Germany), the tibiae were cut into two separate sections, defining metaphyseal and cortical sections. A metaphyseal section was obtained by transversally cutting 2 cm of the proximal condyle to expose the trabecular bone. A second frontal cut was then made through the proximal condyle to define the metaphyseal tibia. The diaphyseal cortex was defined by a 1-cm transversal section of the central tibiae, approximately 5–6 cm from the distal end of the tibia. Samples were stored in 70% ethanol. Investigators were blinded to the allocation of the bone samples in treatment groups.

2.3. Histomorphometry of trabecular and cortical bones

Longitudinal sections (6-μm) were cut on a Leica SM 2500S sledge microtome (Leica Biosystems, Heidelberg, Germany) and mounted on glass slides (Fisher Scientific, Pittsburgh, PA, USA). Coverslips were applied using Eukitt's mounting media (EMS, Ft. Washington, PA, USA). For cortical bone histomorphometry of the central tibia, bone specimens were processed as described above, followed by embedding in 90% methyl methacrylate/10% dibutyl phthalate. Cross sections of 120-μm thickness were collected.

For the lumbar vertebrae (LV6), measurements were made in a 3 × 4-mm area of interest (ROI) of the 1/3 caudal aspect of the plane of section placed about 1 mm from the end plate and centered between the dorsal and ventral sides. All histomorphometric measurements for bone specimens were performed on a light/epifluorescent microscope, Nikon Eclipse 80i (Nikon Instruments, Melville, NY, USA) equipped with an Optonics DEI-750 CE (Tuttlingen, Germany) video camera interfaced to an image analysis system (Bioquant R&M Biometrics, Nashville, TN, USA). All measurements and calculations of dynamic histomorphometry for trabecular and cortical bones followed a standard method as previously described (Dempster et al., 2013).

Dynamic indices were measured in all samples except in four which had to be excluded for measurement of trabecular indices at 12 months of treatment due to wrong labeling schedule. Mineralizing surface (MS/BS, %) was calculated as double plus half the single-labeled surface divided by total bone surface. Thus, in cases where no double labels were found, MS/BS represents the half of the single labeled surface per bone surface. CAL and TCY labeling were measured at trabecular (Tb) surfaces of LV6 and proximal tibiae sites, and at periosteal (Ps) and endocortical (Ec) surfaces of the central tibiae.

2.4. Quantitative backscatter electron imaging (qBEI)

Samples for qBEI measurements were prepared from the same bone specimens used for histomorphometric analysis. Sample blocks were

trimmed using a low speed diamond saw (Isomet-R, Buehler Ltd. Lake Buff, IL, USA). Sectioned bone surfaces were sequentially grinded with sand paper with increasing grid number followed by polishing with diamond grains (size down to 1.0 μm) on hard polishing clothes by a precision polishing device (PM5 Logitech, Glasgow, Scotland). Finally the sample surface was carbon coated by vacuum evaporation (Agar SEM Carbon Coater, Stansted, UK).

The qBEI technique is well established and validated and the details of the method have been published elsewhere (Roschger et al., 2008). Briefly, qBEI makes use of the fact that the intensity of electrons backscattered from a depth of 1.5 μm from the surface-layer of a sectioned bone area is proportional to the weight concentration of mineral (hydroxyapatite/calcium) in bone. A digital electron microscope (DSM 962, Zeiss, Oberkochen, Germany) equipped with a four quadrant semiconductor backscattered electron (BE) detector was used. The BE-signal (gray scale) was calibrated using the "atomic number contrast" between carbon (C, atomic number 6) and aluminum (Al, atomic number 13) as reference materials. Carbon was set to gray level index 25 and Al to 225. This allows a scaling also into weight % (wt%) Ca, whereby, osteoid (atomic number ~ 6) has 0 wt% Ca and pure hydroxyapatite (atomic number 14.06) has 39.86 wt% Ca according to its composition. Thus, one gray level step corresponds to 0.17 wt% Ca as a consequence of this calibration protocol.

Digital calibrated BE-images were acquired with a 50× nominal magnification (resolution 4 μm/pixel) from the sectioned bone areas of selected ROIs (Fig. 1). From these images, gray-level histograms (frequency distributions) were generated indicating the percentage of mineralized bone area (*y*-axis) corresponding to the number of pixels with a certain gray level (*x* axis). Following calibration, the BE-image gray-level distribution can be interpreted as a wt% Ca bone mineralization density distribution (BMDD) for bone tissue. Five BMDD parameters were measured to characterize the BMDD for statistical analysis (Roschger et al., 2003):

1) CaMean is the weighted average Ca concentration of the mineralized tissue area, obtained from the integrated area under the BMDD curve.
2) CaPeak is the peak position of the BMDD histogram showing the most frequently occurring wt% Ca of the measured areas.
3) CaWidth is the width at half-maximum of the BMDD histogram peak indicating the heterogeneity of mineralization.
4) CaLow is the fraction of lowly mineralized tissue area (below 17.68 wt% Ca which is the 5th percentile of trabecular bone from a

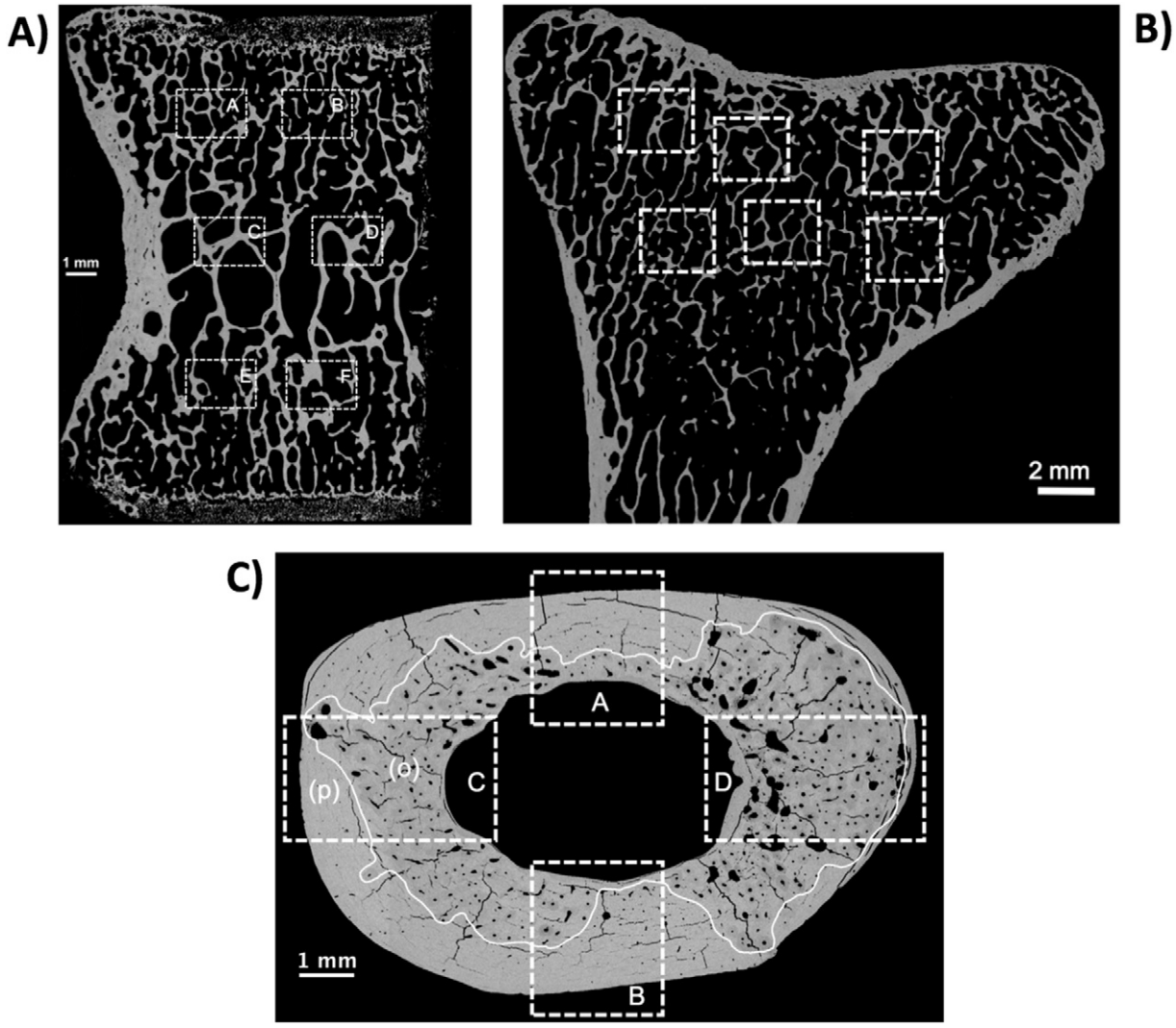

Fig. 1. Examples of qBEI overview images of the bone sections analyzed. The regions of interest are indicated by white boxes (dashed lines). A) Half vertebral frontal section (ventral plane) with six ROIs: 2 central (C and D), and 4 zones closer to the vertebral endplates (A, B, E, F). B) Longitudinal front section of proximal metaphyseal bone of tibia. Central region were analyzed by 6 ROIs. C) Transversal section of tibial midshaft cortex with four ROIs: A and B in the sector of the minor axis of the ellipsoidal cortical cross sectional area and C and D in the sector of the long axis of cross section. These ROIs were divided into primary (p) and osteonal (o) bone regions for separate analysis.

human adult reference BMDD data base (Roschger et al., 2003) and indicates the percentage of primary mineralized areas in human bone).

5) CaHigh indicates the fraction of area of highly mineralized bone tissue (>25.30 wt% calcium which is the 95th percentile of trabecular bone from a human adult reference BMDD data base (Roschger et al., 2003).

2.5. Correlation of BMDD parameters with histomorphometric dynamic indices of bone turnover

For the correlation analyses, data from all animal groups (INT, VEH, ODN-L, ODN-H, ALN) were considered. For correlation in vertebral trabecular bone, 5 samples had to be omitted (n = 2 INT, n = 2 ODN-L, n = 1 ODN-H) due to the occurrence of local/focal abnormal features typical for hyperostosis; note that the local abnormalities are not specific to any group. Hyperostosis is a form of degradation, relatively commonly found in vertebral bone from aged rhesus monkeys (Swezey et al., 1991) and characterized by local increased bone resorption and extensive new bone apposition on the surface of the pre-existing bone motifs. The latter affects local bone matrix mineralization at the site of hyperostosis. As these focal changes in bone matrix mineralization were not representative for the entire sample, these areas of abnormal bone formation were carefully excluded for BMDD in the mentioned n = 5 samples (i.e. none of the ROIs of BMDD measurement as indicated in Fig. 1 contained areas of hyperostosis). Moreover, these 5 samples mentioned were excluded from Tb.MS/BS comparison among the study groups (Table 2) and the analysis of correlation with BMDD outcomes (Table 3, Fig. 4).

2.6. Assessment of relative percentage of primary vs. osteonal bone area in tibial cross-sections

Stitching of the digital backscatter electron images acquired at a nominal magnification of 12× (pixel resolution 9 μm/pixel) was used for receiving overview images of the entire area of the tibial cross-sections. In these images osteonal areas (areas of secondary osteons, osteonal B·Ar) and primary bone areas (devoid of secondary osteons, prim. B·Ar) were identified throughout by the same experienced observer (PM). An example of a cross-sectional area with indicated osteonal and primary bone area is shown in Fig. 1C. The number of pixels for osteonal and primary bone were used for the calculation of percentage of primary bone as follows:

$$\%\text{prim.B.Ar} = 100 \times [\text{prim.B.Ar}/(\text{prim.B.Ar} + \text{osteonal B.Ar})]$$

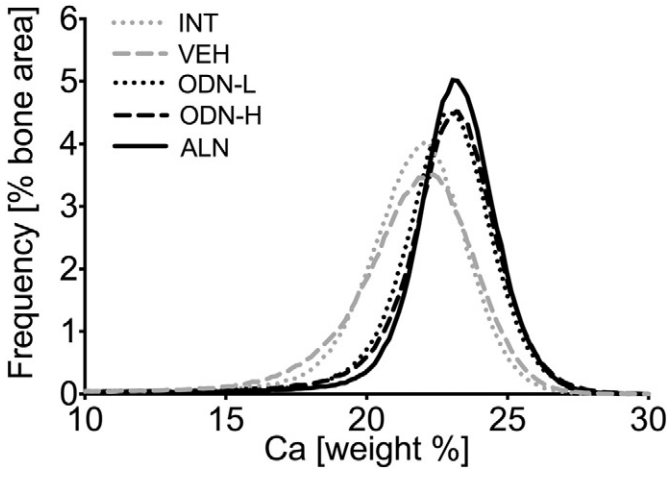

Fig. 2. Representative examples of treatment effects on vertebral cancellous bone: a representative BMDD per study group (INT, VEH, ODN-L, ODN-H and ALN).

2.7. Statistical analysis

All results are shown as the mean ± standard deviation (SD) or median (25th, 75th percentiles) for normally or non-normally distributed data, respectively. Differences among the four study groups were analyzed by one way analysis of variance (ANOVA) or non-parametric Kruskal-Wallis ANOVA on ranks (latter for non-normally distributed data), followed by Fisher LSD post-hoc or Dunn's multiple comparison. Correlation analyses are based on Spearman rank order correlation or Pearson Product moment correlation. Statistical significance was considered at $p < 0.05$.

3. Results

Fig. 1 shows the regions of interest (ROIs) for BMDD measurements at four different skeletal sites (vertebral trabecular bone, tibial metaphyseal trabecular bone, osteonal tibial midshaft bone, and primary tibial midshaft bone) of animals from INT (not included in the original randomization) and study groups VEH, ODN-L, ODN-H, and ALN. One example of tibial cortical bone is shown to demonstrate the separation of osteonal and primary tibial bone (Fig. 1C).

(A) Treament effects in trabecular BMDD of L6 vertebra and proximal tibia

Treatment with ODN-L, ODN-H or ALN significantly affected the BMDD of trabecular bone. One representative example of trabecular vertebral BMDD of each treatment group (VEH, ODN-L, ODN-H, ALN) is shown in Fig. 2. For instance the BMDD of ODN-L was clearly shifted to higher mineralization densities with respect to VEH, which was also

Table 1
BMDD results from trabecular and cortical sites of all treatment groups.

			Treatment groups				
		INT[a]	VEH	ODN–L	ODN–H	ALN	p–Value
Vertebral trabecular	CaMean [wt%]	21.09 (0.66)	20.95 (0.51)	22.31*** (0.38)	22.22 *** (0.82)	22.36*** (0.68)	<0.001
	CaPeak [wt%]	22.12 (0.72)	21.90 (0.49)	23.07 *** (0.42)	23.03*** (0.75)	23.08*** (0.71)	0.001
	CaWidth [Δwt%]	4.01 (0.44)	4.29 (0.69)	3.34 *** (0.39)	3.62 ** (0.29)	3.26*** (0.14)	<0.001
	CaLow [%]	9.01 (2.91)	9.34 (2.93)	5.66*** (0.87)	5.92*** (1.03)	5.01*** (0.37)	<0.001
	CaHigh [%]	3.11 (2.17)	2.63 (1.94)	8.10 (3.86)	9.85 (7.53)	8.69 (6.57)	n.s. (0.058)
Metaphyseal trabecular	CaMean [wt%]	22.09 (0.50)	21.30 (0.82)	22.15 ** (0.43)	22.45 *** (0.34)	22.46*** (0.24)	<0.001
	CaPeak [wt%]	23.01 (0.57)	22.20 (0.65)	22.88 ** (0.43)	23.24 *** (0.22)	23.02** (0.34)	<0.001
	CaWidth [Δwt%]	3.44 (0.27)	3.60 (0.37)	3.18 ** (0.26)	3.21 ** (0.21)	3.18** (0.21)	0.013
	CaLow [%]	5.77 (1.05)	7.48 (3.01)	5.45 * (0.91)	5.59 (1.97)	4.03** (0.28)	0.022
	CaHigh [%]	6.16 (4.52)	2.50 (1.92)	5.53*# (3.53)	8.18*** (1.85)	5.96* (2.42)	0.002
Osteonal cortical	CaMean [wt%]	24.56 (0.53)	24.05 (0.51)	24.39* (0.33)	24.58* (0.36)	24.89*** (0.27)	0.004
	CaPeak [wt%]	25.24 (0.45)	25.04 (0.56)	25.09 (0.27)	25.28 (0.45)	25.45 (0.37)	n.s.
	CaWidth [Δwt%]	3.27 (0.36)	3.64 (0.70)	3.16 (0.37)	3.12 (0.31)	3.44 0.37	n.s.
	CaLow [%]	2.56 (0.59)	3.34 (0.69)	2.75* (0.44)	2.99 (0.45)	2.45** (0.26)	0.018
	CaHigh [%]	45.97 (12.0)	37.95 (11.63)	41.17 (8.99)	47.56 (12.62)	52.69 (8.54)	n.s. (0.071)
Primary cortical	CaMean [wt%]	25.62 (0.43)	25.36 (0.54)	25.27 (0.50)	25.19 (0.61)	25.70 (0.41)	n.s.
	CaPeak [wt%]	26.00 (0.51)	25.76 (0.39)	25.82 (0.51)	25.74 (0.60)	26.17 (0.44)	n.s.
	CaWidth [Δwt%]	2.60 (2.43; 2.60)	2.25 (2.25; 2.43)	2.43 (2.34; 2.60)	2.25 (2.25; 2.51)	2.69 (2.43; 2.77)	n.s.
	CaLow [%]	1.97 (0.24)	2.08 (0.61)	2.09 (0.44)	2.56 (0.49)	2.19 (0.25)	n.s.
	CaHigh [%]	72.85 (11.05)	67.99 (13.44)	64.88 (11.99)	64.87 (19.40)	74.95 (10.34)	n.s.

Data are mean (SD) or median (25th; 75th percentiles). p–Value is based on ANOVA or non–parametric Kruskal–Wallis comparison between treatment groups.
[a]No statistical comparison to INT was performed.
***p ≤ 0.001, **p < 0.01, *p < 0.05 vs. VEH based on post–hoc Fischer LSD method
#p < 0.05 vs. ODN–H based on post–hoc Fischer LSD method

accompanied by a reduction in the width of the BMDD-peak. Similar changes of BMDD curves could be observed also for ODN-H and ALN (Fig. 2).

Statistical comparison of the four treatment groups revealed significant differences in all trabecular BMDD derived parameters at both sites, vertebra and tibia. Corresponding ANOVA or ANOVA on ranks and post-hoc tests are summarized in Table 1. Percent differences of all trabecular BMDD parameters in the study groups to VEH mean are shown in Fig. 3. In particular, CaMean and CaPeak of trabecular bone in vertebrae and proximal tibia bone were significantly higher in ODN-L (CaMean: +6.5%, $p < 0.001$ and +4.0%, $p < 0.01$), ODN-H (CaMean: +6.1%, $p < 0.001$ and +5.4%, $p < 0.001$), and ALN treated groups (CaMean: +6.7%, $p < 0.001$ and +5.4%, $p < 0.001$ for trabecular bone in vertebrae and tibial metaphysis, respectively) compared to VEH, while CaWidth and CaLow were significantly reduced in ODN-L, ODN-H, and ALN treated groups compared to VEH (Table 1).

No significant differences between the BMDD parameters among the groups treated with the bone resorption inhibitors (ODN-L vs. ODN-H vs. ALN), could be detected (all post-hoc tests >0.05) with the exception of metaphyseal tibial CaHigh which was higher in ODN-H compared to ODN-L ($p < 0.05$).

(B) Treatment effects in cortical BMDD in central tibia

Comparison of the four treatment groups revealed significant differences in BMDD from osteonal and no significant differences from those of primary (devoid of secondary osteons) cortical bone of the tibia (corresponding ANOVA or ANOVA on ranks and post-hoc tests are summarized in Table 1). Tibial osteonal CaMean was increased for ODN-L (+1.4%, $p < 0.05$), ODN-H (+2.2%, $p < 0.05$) and ALN treated animals (+3.4%, $p < 0.001$) while tibial osteonal CaLow was decreased for ODN-L (−17.7%, $p < 0.05$) and ALN (−26.6%, $p < 0.01$) compared to VEH treated.

Mean and standard deviation of percentage of primary bone area (%prim. B.Ar) was 41 ± 14% for INT, 40 ± 11% for VEH, 42 ± 4% for ODN-L, 45 ± 13% for ODN-H, and 51 ± 13% for ALN. ANOVA comparison between the treatment groups (comparing VEH, ODN-L, ODN-H, and ALN) showed no significant differences ($p = 0.232$) in % prim. B.Ar.

(C) Treatment effects on mineralizing surface per bone surface and correlation with BMDD parameters

Average levels (median and interquartile range) of trabecular (Tb.MS/BS), periosteal (Ps.MS/BS), and endocortical mineralizing surface per bone surface (Ec.MS/BS) from all study groups and INT animals are shown in Table 2 (INT data were not included for statistical analysis). After 12 and 20 months of treatment, ODN-H and ALN reduced Tb.MS/BS versus VEH. No significant differences among the study groups were observed for Ps.MS/BS or Ec.MS/BS. These parameters, however, revealed a large inter-individual variation within the groups. A high percentage of samples were lacking double labels at both 12 months and 20 months of treatment. Details on the number of samples with double labels are shown in Table 2.

Regression analyses between Tb.MS/BS and BMDD variables were performed for all groups (INT, VEH, ODN-L, ODN-H, ALN) or only with the ovariectomized study groups (Table 3). Highly significant

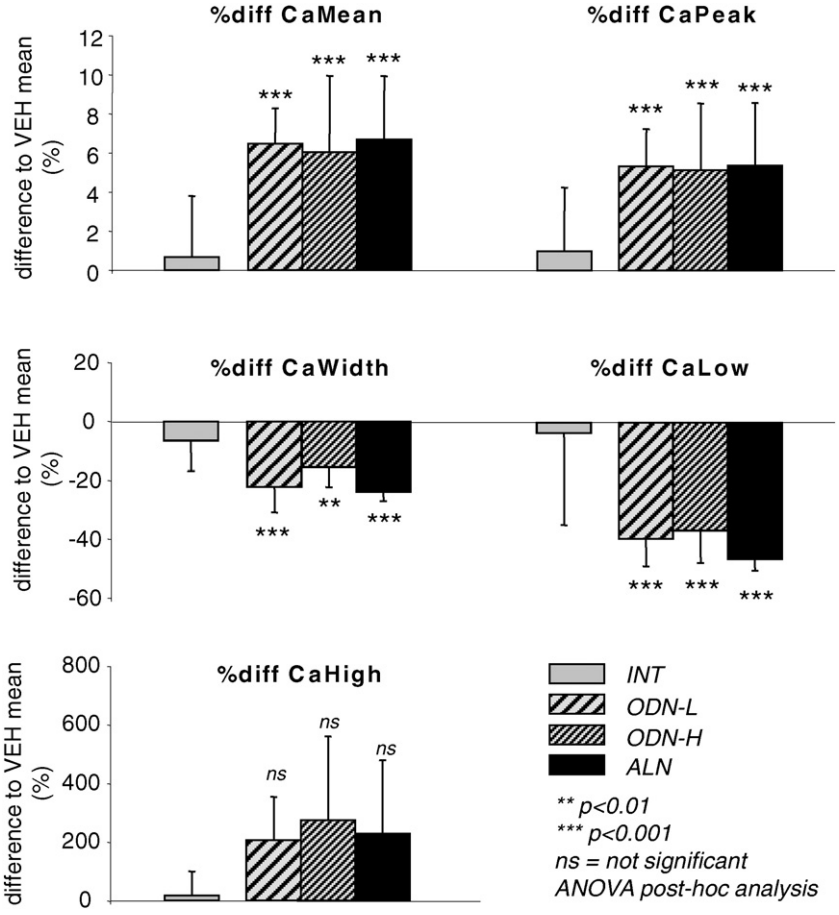

Fig. 3. Effects of 20 months treatment on BMDD of vertebral trabecular bone. The differences to VEH mean are shown for INT (gray), ODN-L (light gray, coarse shaded), ODN-H (light gray, fine shaded), and ALN (black). Bars indicate mean ± SD. * $p < 0.05$,** $p < 0.01$, *** $p < 0.001$ versus VEH (ANOVA post-hoc tests from Table 1).

correlations of Tb.MS/BS based on calcein labels (reflecting bone formation rate at 12 months treatment) with BMDD parameters were found in vertebral trabecular bone (Table 3). Similarly, correlations with Tb.MS/BS based on tetracycline labels (reflecting bone formation rate at 20 months treatment) could be observed (Table 3). Vertebral trabecular CaMean plotted versus Tb.MS/BS at 12 months and at 20 months is shown in Fig. 4 (statistical outcomes with and without the INT group are shown).

Regression analysis between central cortical tibial Ps.MS/BS or Ec.MS/BS with BMDD outcomes including all animal groups revealed no significant relationship with the exception of a significant correlation between primary cortical bone CaLow and Ec.MS/BS based on calcein labels ($R = 0.39$, $p = 0.02$). This correlation remained statistically significant if the INT group was omitted from analysis ($R = 0.37$, $p = 0.04$). Moreover, no significant correlations between primary bone areas (%prim. B.Ar) and bone formation at the tibiae (Ps.MS/BS, Ec.MS/BS) could be observed.

4. Discussion

We have studied the effects of 20 months treatment with ODN-L or ODN-H head to head comparison to ALN on the bone matrix mineralization in OVX adult rhesus monkeys. For this study, bone samples were obtained from animals treated with two doses of ODN at ~1.8 fold (ODN-L) and ~7.8 fold (ODN-H) clinical exposure estimated from ODN 50-mg once-weekly and a dose of ALN equivalent to the 70-mg once-week (Williams et al., 2013). We observed a significant shift of the BMDD toward higher mineralization densities in trabecular and osteonal compartments with ODN at both doses and ALN. In contrast, primary bone of the tibiae (devoid of secondary osteons) did not reveal this shift toward higher bone matrix mineralization. Correlation analyses of trabecular bone Tb.MS/BS versus BMDD parameters (both derived from vertebrae) revealed that treatment-related reductions in Tb.MS/BS were correlated with the increases in the degree of mineralization and the decreases in heterogeneity of mineralization.

The observed BMDD outcomes in ODN-L, ODN-H, ALN compared to VEH after 20 months of treatment were completely consistent with the antiresorptive action of a bisphosphonate, as previously reported on treatment with ALN or other antiresorptive agents in bone from postmenopausal osteoporotic women (Roschger et al., 2014). Higher CaMean, CaPeak and CaHigh are indicative for increased average tissue age in treated bone. This is due to a prolonged period of secondary mineralization in the bone structural units (BSUs). Simultaneously, CaLow, the fraction of lowly mineralized bone areas was significantly decreased, as less new BSUs were formed during treatment. Further, CaWidth, the heterogeneity of the matrix mineralization was reduced, which represents a typical transient effect on the BMDD, when the bone turnover rate has dropped to a lower level (Ruffoni et al., 2008; Roschger et al., 2014). Our previous study with ODN dosed at subclinical exposures did not show statistically significant changes in BMDD (Fratzl-Zelman et al., 2013). In the present work, ODN at doses higher than clinical exposures significantly increased secondary mineralization as compared to VEH controls. The dependency of the BMDD outcomes on bone turnover is reflected by the significant correlations of mineralizing surface with BMDD parameters obtained from vertebral trabecular bone.

It is important to note this study was conducted in prevention when drug dosing started 10 days post-OVX (Williams et al., 2013), therefore treatment-related actions on bone occurred during the high remodeling status in skeletal mature monkeys at newly estrogen deficient condition. By comparing ODN to ALN, the effect on trabecular BMDD is very similar for both drugs, although their mechanisms of reduction of bone turnover are very different (Duong, 2012; Reginster et al., 2014).

Table 2
Histomorphometric mineralizing surface per bone surface (MS/BS) in OVX-rhesus monkeys.

Group	Intact[a]	Study groups (OVX)			
		Veh	ODN-L 2 mg/kg/d	ODN-H 4 mg/kg/d	ALN 30 μg/kg/wk
Vertebral trabecular bone at 12 months of treatment					
# samples[b]	6	8	4	6	5
# samples with DL	6	7	3	1	1
# samples with any label	6	8	4	6	3
Tb.MS/BS (%)	3.80 (2.30; 4.90)	8.90 (4.05; 11.70)	1.60 (0.75; 2.55)	0.30 (0.20; 0.30)*	0.50 (0.00; 1.08)*
Vertebral trabecular bone at 20 months of treatment					
# samples[c]	6	8	6	7	6
# samples with DL	6	7	3	2	3
# samples with any label	6	7	3	2	3
Tb.MS/BS (%)	4.92 (2.72; 10.71)	2.95 (1.60; 5.20)	0.02 (0.00; 0.38)	0.00 (0.00; 0.02)*	0.03 (0.00; 0.09)
Tibial cortical bone at 12 months of treatment					
# samples	8	8	8	8	6
# samples with DL at Ps sites	2	5	7	7	5
# samples with any label at Ps sites	2	6	8	7	5
Ps.MS/BS	0.00 (0.00; 0.85)	5.17 (0.50; 12.96)	6.25 (2.49; 39.24)	3.63 (2.94; 8.22)	3.58 (1.48; 11.75)
# samples with DL at Ec sites	6	4	3	5	4
# samples with any label at Ec sites	7	7	8	7	4
Ec.MS/BS	8.72 (0.88; 17.31)	1.52 (0.71; 11.48)	2.52 (0.35; 10.73)	6.46 (1.49; 20.54)	8.22 (0.00; 13.73)
Tibial cortical bone at 20 months of treatment					
# samples	8	8	8	8	6
# samples with DL at Ps sites	3	3	7	5	0
# samples with any label at Ps sites	5	5	7	7	3
Ps.MS/BS	0.35 (0.00; 4.60)	0.43 (0.00; 5.64)	9.96 (0.83; 27.66)	0.87 (0.46; 8.18)	0.31 (0.00; 0.63)
# samples with DL at Ec sites	6	3	3	5	1
# samples with any label at Ec sites	8	6	6	5	4
Ec.MS/BS	5.85 (2.50; 8.60)	1.34 (0.15; 2.58)	0.58 (0.16; 6.36)	3.07 (0.00; 6.94)	0.53 (0.00; 1.91)

Data are median (25th; 75th percentiles).
Tb.MS/BS = trabecular mineralizing surface per bone surface, Ps.MS/BS = periosteal mineralizing surface per bone surface, Ec.MS/BS = endocortical mineralizing surface per bone surface.
* $p < 0.05$ vs. VEH by Dunn's pairwise comparison (following Kruskal-Wallis comparison of median values $p < 0.05$).
[a] Not included in the statistical analysis.
[b] 9 samples had to be excluded (4 due to wrong labeling schedule and 5 due to hyperosteosis).
[c] 5 samples had to be excluded due to hyperosteosis.

Table 3
Pearson product moment correlation analysis of trabecular mineralizing surface per bone surface (MS/BS) versus BMDD parameters obtained from vertebral trabecular compartments.

	12 months labeling		20 months labeling	
L6-vertebra	Tb.MS/BS (n = 29)[a]	Tb.MS/BS (n = 23)[b]	Tb. MS/BS (n = 33)[a]	Tb. MS/BS (n = 27)[b]
CaMean trabecular	R = −0.68, p < 0.001	R = −0.61, p = 0.002	R = −0.43, p = 0.01	R = −0.65, p < 0.001
CaPeak trabecular	R = −0.58, p = 0.001	R = −0.54, p = 0.008	R = −0.35, p = 0.046	R = −0.57, p = 0.002
CaWidth trabecular	R = 0.52 p = 0.004	R = 0.54, p = 0.007	R = 0.48, p = 0.005	R = 0.59, p = 0.001
CaLow trabecular	R = 0.70, p < 0.001	R = 0.67, p < 0.001	R = 0.60, p < 0.001	R = 0.84, p < 0.001
CaHigh trabecular	R = −0.55, p = 0.002	R = −0.42, p = 0.047	R = −0.35, p = 0.048	R = −0.40, p = 0.037

[a] Correlations including samples from all groups (INT, VEH, ODN-L, ODN-H, ALN).
[b] Correlations within OVX-study groups (VEH, ODN-L, ODN-H, ALN).

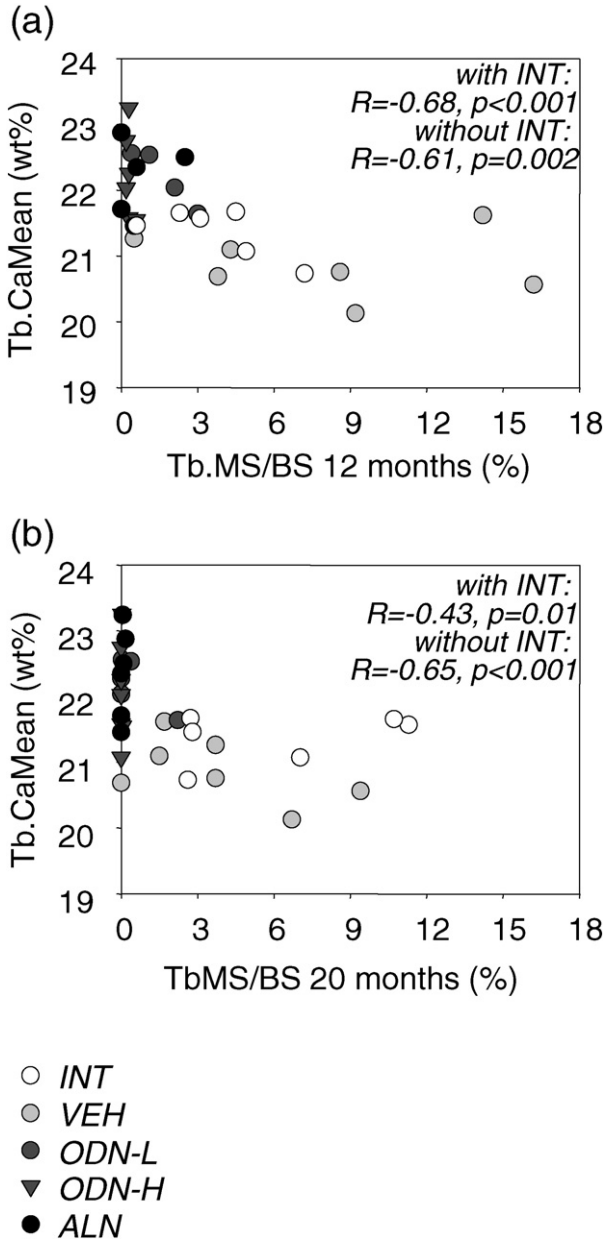

Fig. 4. Correlation of average calcium concentration of vertebral trabecular bone (Tb·CaMean) versus mineralizing surface per bone surface (Tb.MS/BS) ((a) based on calcein (CAL) labels, (b) based on tetracycline (TCY) labels)) measured in the same bone compartment. Correlation outcomes (Spearman rank order correlation coefficient R and corresponding p-value) for all animal groups (INT white, VEH light gray, ODN-L dark gray circle, ODN-H dark gray triangle, and ALN black) and for those without INT are shown.

Further, our findings suggest that the effects of ODN at both doses on Tb·BMDD appeared to reach a saturation level after 20-months of treatment. There were no differences among the ODN treatment groups that could be detected for any Tb·BMDD parameter at the four measured sites with the exception of lower metaphyseal trabecular CaHigh in the ODN lower compared to ODN higher dose group. The similarity of the Tb·BMDD effects in ODN at both doses and ALN groups might be due to the fact that bone turnover is highly reduced in trabecular and osteonal compartments, consistent with the Tb.MS/BS levels near zero after 20 months of treatment in both ODN and ALN groups. Strong treatment-related reductions of Tb.MS/BS, particularly in the ODN-L (~1.8-fold clinical exposure) and ALN groups (equivalent to clinical exposure), were evident. The observed reduction in Tb.MS/BS is consistent with the changes in bone turnover markers at 18 months of treatment reported for the same monkeys (Williams et al., 2013). Urinary amino-terminal telopeptides (uNTx) and serum N-propeptide of type 1 collagen (sP1NP) decreased by about −80% and −50%, respectively in ODN-L and by −80% (for both markers) in the ALN group (Williams et al., 2013) compared to VEH.

Tibial diaphyseal central cortical bone of these skeletally mature rhesus monkeys is highly heterogeneous, consisting of compact, highly mineralized, primary bone (devoid of secondary osteons), which is co-existing with secondary osteonal bone. Osteonal bone represents bone areas with intracortical remodeling. Assessment of the percentages of primary or osteonal bone areas in the tibial diaphyseal cross-sections showed that neither parameter was changed by treatment, suggesting that ODN or ALN treatment did not change the relative amount of area/volume of intracortical remodeling in the tibial shaft of the monkeys.

Given our selection criterion for primary bone (devoid of secondary lower mineralized osteons), our BMDD findings revealed that the average degree of mineralization (CaMean, Table 2) is numerically higher than that in osteonal bone in all groups, which is consistent with a higher average tissue age in primary bone independent of treatment. Moreover, in osteonal bone, the shift toward higher bone mineralization densities induced by ODN or ALN treatment similar to that in trabecular compartments was observed. This is consistent with the treatment-related inhibition of bone resorption effect on intracortical bone remodeling as previously reported previously in femoral shaft of the OVX-rhesus monkeys (Cusick et al., 2012). The lack of treatment effects on the BMDD in primary cortical bone suggests low bone turnover/formation activity at this site. In general, significant periosteal bone formation would have been expected to have an impact on the BMDD, i.e. to decrease the average mineralization densities due to the presence of younger bone matrix. Periosteal and endocortical MS/BS measured in cortical bone of the tibia revealed a large variation between the animals within each group, pointing toward a high intra-individual site-specific variation in bone modelling. Further, one might speculate that the observation of unchanged primary cortical BMDD does not necessarily exclude the possibility of periosteal bone formation as mineralization of newly formed bone areas might occur faster at periosteal sites (Wergedal and Baylink, 1974) and too rapidly for an impact on the BMDD. However, dynamic histomorphometry demonstrated there was no treatment related changes detected in periosteal bone formation

of the tibia in the ODN groups or ALN. This finding seems to limit to the tibial diaphysis, since significant periosteal bone formation was previously reported in ODN-treated femoral sites, including femoral neck, proximal femur and central femur in OVX-rhesus monkeys (Cusick et al., 2012).

In summary, ODN dosed in prevention mode at supraclinical exposures increased the degree and reduced the heterogeneity of bone matrix mineralization in trabecular and intra-cortical (osteonal) compartments. The similarity of the BMDD effects at both ODN doses indicates that the maximum effect of this drug on BMDD is already achieved at the lower (~ 1.8 fold clinical exposure) dose after 20-months of treatment. The overall treatment-related effects on BMDD in the spine and tibia were similar to those of ALN and are in line with the effect of ODN on blocking bone resorption.

Disclosure statement

BMM, PR, PM, and KK have nothing to declare. CC, MP, and LTD are employees of Merck &Co.

Acknowledgements

The authors thank Daniela Gabriel, Petra Keplinger, and Sonja Lueger for sample preparation at the Bone Material Laboratory of the Ludwig Boltzmann Institute of Osteology, Vienna, Austria. This work was supported by the AUVA (Austrian Social Insurance for Occupational Risk) and the WGKK (Social Health Insurance Vienna), and received financial support by Merck.

References

Bone, H.G., Dempster, D.W., Eisman, J.A., Greenspan, S.L., McClung, M.R., Nakamura, T., Papapoulos, S., Shih, W.J., Rybak-Feiglin, A., Santora, A.C., Verbruggen, N., Leung, A.T., Lombardi, A., 2015. Odanacatib for the treatment of postmenopausal osteoporosis: development history and design and participant characteristics of LOFT, the long-term odanacatib fracture trial. Osteoporos. Int. 26 (2), 699–712. http://dx.doi.org/10.1007/s00198-014-2944-6 (Feb).

Brixen, K., Chapurlat, R., Cheung, A.M., Keaveny, T.M., Fuerst, T., Engelke, K., Recker, R., Dardzinski, B., Verbruggen, N., Ather, S., Rosenberg, E., de Papp, A.E., 2013. Bone density, turnover, and estimated strength in postmenopausal women treated with odanacatib: a randomized trial. J. Clin. Endocrinol. Metab. 98 (2), 571–580. http://dx.doi.org/10.1210/jc.2012-2972 (Feb).

Cabal, A., Jayakar, R.Y., Sardesai, S., Phillips, E.A., Szumiloski, J., Posavec, D.J., Mathers, P.D., Savitz, A.T., Scott, B.B., Winkelmann, C.T., Motzel, S., Cook, L., Hargreaves, R., Evelhoch, J.L., Dardzinski, B.J., Hangartner, T.N., McCracken, P.J., Duong, L.T., Williams, D.S., 2013. High-resolution peripheral quantitative computed tomography and finite element analysis of bone strength at the distal radius in ovariectomized adult rhesus monkey demonstrate efficacy of odanacatib and differentiation from alendronate. Bone 56 (2), 497–505. http://dx.doi.org/10.1016/j.bone.2013.06.011 (Oct).

Chapurlat, R.D., 2015. Odanacatib: a review of its potential in the management of osteoporosis in postmenopausal women. Ther. Adv. Musculoskelet. Dis. 7 (3), 103–109. http://dx.doi.org/10.1177/1759720X15580903 s(Review, Jun).

Cheung, A.M., Majumdar, S., Brixen, K., Chapurlat, R., Fuerst, T., Engelke, K., Dardzinski, B., Cabal, A., Verbruggen, N., Ather, S., Rosenberg, E., de Papp, A.E., 2014. Effects of odanacatib on the radius and tibia of postmenopausal women: improvements in bone geometry, microarchitecture, and estimated bone strength. J. Bone Miner. Res. 29 (8), 1786–1794. http://dx.doi.org/10.1002/jbmr.2194 (Aug).

Currey, J.D., 2004. Tensile yield in compact bone is determined by strain, post-yield behaviour by mineral content. J. Biomech. 37, 549–556.

Cusick, T., Chen, C.M., Pennypacker, B.L., Pickarski, M., Kimmel, D.B., Scott, B.B., Duong, L.T., 2012. Odanacatib treatment increases hip bone mass and cortical thickness by preserving endocortical bone formation and stimulating periosteal bone formation in the ovariectomized adult rhesus monkey. J. Bone Miner. Res. 27, 524–537.

Dempster, D.W., Compston, J.E., Drezner, M.K., Glorieux, F.H., Kanis, J.A., Malluche, H., Meunier, P.J., Ott, S.M., Recker, R.R., Parfitt, A.M., 2013. Standardized nomenclature, symbols, and units for bone histomorphometry: a 2012 update of the report of the ASBMR Histomorphometry Nomenclature Committee. J. Bone Miner. Res. 28, 2–17.

Duong, L.T., 2012. Therapeutic inhibition of cathepsin K-reducing bone resorption while maintaining bone formation. Bonekey Rep. 1, 67. http://dx.doi.org/10.1038/bonekey.2012.67 (eCollection 2012, May 2).

Duong, L.T., Leung, A.T., Langdahl, B., Cathepsin, K., 2015. Inhibition: a new mechanism for the treatment of osteoporosis. Calcif. Tissue Int. ([Epub ahead of print], Sep 3).

Fratzl, P., Gupta, H.S., Paschalis, E.P., Roschger, P., 2004. Structure and mechanical quality of the collagen-mineral nano-composite in bone. J. Mater. Chem. 14, 2115–2123.

Fratzl-Zelman, N., Roschger, P., Fisher, J.E., Duong le, T., Klaushofer, K., 2013. Effects of odanacatib on bone mineralization density distribution in thoracic spine and femora of ovariectomized adult rhesus monkeys: a quantitative backscattered electron imaging study. Calcif. Tissue Int. 92 (3), 261–269 (Mar).

Jensen, P.R., Andersen, T.L., Pennypacker, B.L., Duong, L.T., Delaissé, J.M., 2014. The bone resorption inhibitors odanacatib and alendronate affect post-osteoclastic events differently in ovariectomized rabbits. Calcif. Tissue Int. 94 (2), 212–222. http://dx.doi.org/10.1007/s00223-013-9800-0 (Epub 2013 Oct 2, Feb).

Masarachia, P.J., Pennypacker, B.L., Pickarski, M., Scott, K.R., Wesolowski, G.A., Smith, S.Y., Samadfam, R., Goetzmann, J.E., Scott, B.B., Kimmel, D.B., LT, Duong, 2012. Odanacatib reduces bone turnover and increases bone mass in the lumbar spine of skeletally mature ovariectomized rhesus monkeys. J. Bone Miner. Res. 27 (3), 509–523. http://dx.doi.org/10.1002/jbmr.1475 (Mar).

Pennypacker, B.L., Duong, L.T., Cusick, T.E., Masarachia, P.J., Gentile, M.A., Gauthier, J.Y., Black, W.C., Scott, B.B., Samadfam, R., Smith, S.Y., Kimmel, D.B., 2011. Cathepsin K inhibitors prevent bone loss in estrogen-deficient rabbits. J. Bone Miner. Res. 26 (2), 252–262. http://dx.doi.org/10.1002/jbmr.223 (Feb).

Pennypacker, B.L., Chen, C.M., Zheng, H., Shih, M.S., Belfast, M., Samadfam, R., Duong, L.T., 2014. Inhibition of cathepsin K increases modeling-based bone formation, and improves cortical dimension and strength in adult ovariectomized monkeys. J. Bone Miner. Res. 29 (8), 1847–1858. http://dx.doi.org/10.1002/jbmr.2211 (Aug).

Reginster, J.Y., Neuprez, A., Beaudart, C., Lecart, M.P., Sarlet, N., Bernard, D., Disteche, S., Bruyere, O., 2014. Antiresorptive drugs beyond bisphosphonates and selective oestrogen receptor modulators for the management of postmenopausal osteoporosis. Drugs Aging 31, 413–424.

Roschger, P., Gupta, H.S., Berzlanovich, A., Ittner, G., Dempster, D.W., Fratzl, P., Cosman, F., Parisien, M., Lindsay, R., Nieves, J.W., Klaushofer, K., 2003. Constant mineralization density distribution in cancellous human bone. Bone 32, 316–323.

Roschger, P., Paschalis, E.P., Fratzl, P., Klaushofer, K., 2008. Bone mineralization density distribution in health and disease. Bone 42, 456–466.

Roschger, P., Misof, B., Paschalis, E., Fratzl, P., Klaushofer, K., 2014. Changes in the degree of mineralization with osteoporosis and its treatment. Curr. Osteoporos. Rep. 12, 338–350.

Ruffoni, D., Fratzl, P., Roschger, P., Phipps, R., Klaushofer, K., Weinkamer, R., 2008. Effect of temporal changes in bone turnover on the bone mineralization density distribution: a computer simulation study. J. Bone Miner. Res. 23, 1905–1914.

Stoch, S.A., Zajic, S., Stone, J., Miller, D.L., Van Dyck, K., Gutierrez, M.J., De Decker, M., Liu, L., Liu, Q., Scott, B.B., Panebianco, D., Jin, B., Duong, L.T., Gottesdiener, K., JA, Wagner, 2009. Effect of the cathepsin K inhibitor odanacatib on bone resorption biomarkers in healthy postmenopausal women: two double-blind, randomized, placebo-controlled phase I studies. Clin. Pharmacol. Ther. 86 (2), 175–182.

Swezey, R.L., Cox, C., Gonzales, B., 1991. Ankylosing spondylitis in nonhuman primates: the drill and the siamang. Semin. Arthritis Rheum. 21 (3), 170–174 (Dec).

Thompson, D.D., Seedor, J.G., Quartuccio, H., Solomon, H., Fioravanti, C., Davidson, J., Klein, H., Jackson, R., Clair, J., Frankenfield, D., et al., 1992. The bisphosphonate, alendronate, prevents bone loss in ovariectomized baboons. J. Bone Miner. Res. 7 (8), 951–960.

Wergedal, J.E., Baylink, D.J., 1974. Electron microprobe measurements of bone mineralization rate in vivo. Am. J. Physiol. 226, 345–352.

Williams, D.S., McCracken, P.J., Purcell, M., Pickarski, M., Mathers, P.D., Savitz, A.T., Szumiloski, J., Jayakar, R.Y., Somayajula, S., Krause, S., Brown, K., Winkelmann, C.T., Scott, B.B., Cook, L., Motzel, S.L., Hargreaves, R., Evelhoch, J.L., Cabal, A., Dardzinski, B.J., Hangartner, T.N., Duong, L.T., 2013. Effect of odanacatib on bone turnover markers, bone density and geometry of the spine and hip of ovariectomized monkeys: a head-to-head comparison with alendronate. Bone 56 (2), 489–496. http://dx.doi.org/10.1016/j.bone.2013.06.008 (Oct).